

Numerical Study of Turbulent Flow in Pipe with Sudden Expansion

M. K. Wong, L. C. Sheng, C. S. Nor Azwadi, G. A. Hashim*

Faculty of Mechanical Engineering, University Technology Malaysia, UTM Skudai, 81310
Johor, Malaysia
ghasaq_88@yahoo.com

Abstract – *The turbulent fluid flow through sudden expansion duct studies raise the knowledge of scientific and contribute many practical applications. The sudden change in the surface geometry of the duct cause the severe pressure gradient, the boundary layer separates at the step edge and forms a recirculation zone. The knowledge about the recirculation zone is useful in study turbulent flow properties. This paper presents a numerical study of 2D turbulence flow was modeled by the standard $k-\epsilon$, realizable $k-\epsilon$, and shear stress transport (SST) $k-\omega$ models. The stimulation was conducted by a sudden expansion duct with Reynolds number of 20000 at the inlet of the solution and expansion ratio of 1:2. In this research, flow characteristics at the recirculation zone in the sudden expansion pipe are analyzed. The recirculation size, velocity profile and turbulent intensity are compared between three models of turbulence flow. The results show that SST $k-\omega$ model has the best prediction of separation flow compared to two others models. Furthermore, the trends of mean velocity of these three models are same as the experimental results. Copyright © 2015 Penerbit Akademia Baru - All rights reserved.*

Keywords: Sudden expansion of duct, Turbulent flow and modelling, Flow separation, Recirculation

1.0 INTRODUCTION

In this paper, the turbulent flow in a pipe with sudden expansion geometry is investigated. Flow over sudden expansion geometry generates vortices due to the separation flow resulted from the sudden pressure change in the fluid. The research of flow separation from the surface of a solid body, and the study of global changes in the flow field that develop as a result of the separation are among the most difficult problems and fundamental of fluid dynamics. Flow separation occurs when the boundary layer travels far enough against an adverse pressure gradient that the speed of the boundary layer relative to the object falls almost to zero [1-2].

Turbulent flow separation occurs in many flow situations in industrial and nature. Variable pressure gradients are generated due to varies in the geometry of the flow boundaries by introducing flow separation. The recirculation flow with separation causes enhancement of turbulence, high pressure loss, and increase heat and mass transfer rate. The condition for flow separation to occur is the unfavourable pressure gradient. There are two types of flow separation, separation at internal flow and that in external flow [3]. Separation flows are widely used in industrial applications even though there is still lack of knowledge about information of the flow around the recirculation area [4].

From the classical concept, viscosity induces flow separation; it is recognized as boundary layer separation [5]. Boundary layer separation occurs when the section of boundary layer closest to the wall or leading edges reverses in flow direction. The separation point is the area between the backward and forward flow, where the shear stress is zero. The overall boundary layer initially thickens suddenly at the separation point and is then forced off the surface by the reversed flow at its bottom [6].

The separation reattached flows are characterized by the interaction between eddies and the solid surface. Meanwhile, the separated flow without reattachment is characterized by the interaction between eddies shed from the separation points [7]. Among those who have studied experimentally separating and reattaching flows are Khezzar et al. [8], Back and Roshke [9], Stieglmeier et al. [10], Founti and Klipfel [11], and Driver and Seegmiller [12]. Among those who have studied the phenomenon numerically are Celenligil and Mellor [13], they solved the unsteady governing equations and modelled the flow with a full Reynolds-stress model.

The flow separation condition is relevant to some engineering applications, such as flow over airfoils at large angles of attack, in channels where area suddenly increases, in wide angle diffusers [14-15]. Furthermore, the famous application of the separation flow is the turbulent fluid flow through sudden expansion passage.

Flows through sudden expansion geometries are of interest from the point of view of fundamental fluid mechanics and many practical applications. The turbulent fluid flows through sudden expansion duct are common in several engineering applications such as dump combustor, pipe line, nuclear reactor and heat exchanger. On the fundamental fluid mechanics view, the flow through an axi-symmetric sudden expansion has all the complexities of internally separating and reattaching flows.

The turbulent axi-symmetric sudden expansion flow has been investigated both numerically and experimentally by many researchers. Laufer [16] conducted the first experiment on the fully developed turbulent flow in a circular duct. Vasilev et al. [17] numerically computed the turbulent flow in the sudden expansion of the duct. Launder et al. [18] numerically studied the turbulent flow in a circular duct. Chaurvedi [19] investigated and analyzed the flow characteristics in the axi-symmetric expansion by using the modified standard $k-\varepsilon$ model for streamline curvature. Smyth [20] experimentally studied the turbulent flow with separation and recirculation over the plane symmetric sudden expansion for the Reynolds number of 30,210. Gould et al. [21] examined the turbulent transport in the axisymmetric sudden expansion. Mohanarangam et al. [22] conducted the numerical investigation for turbulent gas-particle flow, to study the effects of particle dispersion and its influence on step heights.

Several configurations of sudden expansion of the axial development of the mean velocities and turbulence quantities has been studied experimentally [23-26]. The behaviour of a suddenly expanding axisymmetric flow in the turbulent regime has also been investigated numerically with a discussion of the reattachment length [27], growth of azimuthal structures [28], and self-sustained precession of the flow field [29]. Armaly et al [30] had investigated about the dependence of the separation length on the Reynolds number. Stieglmeier et al. [31] and Coleet et al. [32] experimentally studied the turbulent fluid flow through the axi-symmetric expansions. Gagnon et al. [33] investigated unsteady recirculating flows in sudden expansions at high Reynolds number. Signrdson [34],

studied the structure and control of a re attaching flow. De Zilwa et al. [35], numerically simulated the turbulent flows in the downstream of the plane sudden expansion by using $k-\epsilon$ turbulent model. Canabzoglu and Bozkir [36], analyzed pressure distribution of turbulent asymmetric flow in a flat duct symmetric sudden expansion experimentally.

2.0 METHODOLOGY

2.1 Design Description

Sudden expansion geometry was tested in 2D. In this simulation, the configuration as considered is shown in Figure 1 where the dimension of geometry was according to Koronaki and Liakos [37]. The sudden expansion geometry consists of a cylindrical duct of diameter $D=0.051\text{m}$ and length $L=1\text{m}$. The expansion ratio is 1:2 and the Reynolds number at the inlet of the solution field is 20000. Intensive study has been done in order to achieve grid independency and as a result a mesh of 12500 (25x500) grid points was found to be adequate for that purpose. Figure 2 shows the mesh grid points. The working fluid is diesel liquid and the physical characteristics of the fluid are listed in Table 1.

Table 1: Fluid properties and flow characteristics

Density	750 kg/m ³
Dynamic Viscosity	0.0024 kg/ms
Maximum Velocity	2.579 m/s

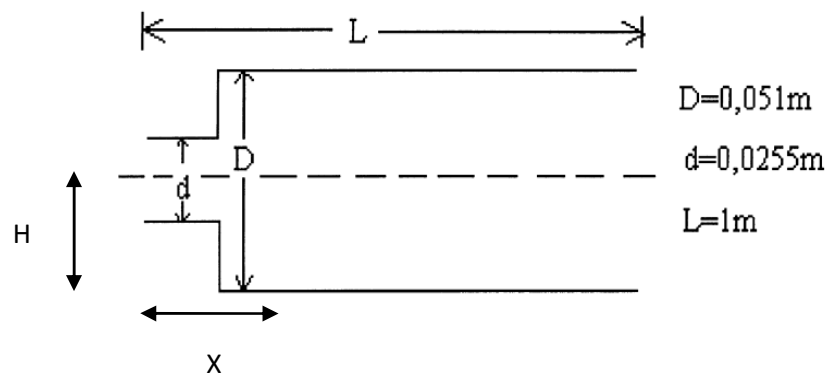


Figure 1: Schematic of the pipe with sudden expansion

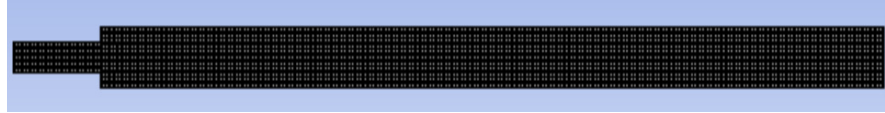


Figure 2:Schematic of 12500 of mesh grid points

2.2 Governing equations

The governing equations of Computational Fluid Dynamics methods are described based on three fundamental equations:

(a) Continuity equations

(b) Momentum equations

(c) Energy equations

The sudden expansion geometry described in this study is in 2 Dimensional. The respective equations of the three fundamental equations are given as follows:

Continuity equation:

$$\frac{\partial U}{\partial X} + \frac{\partial V}{\partial Y} = 0 \quad (1)$$

Momentum equation:

$$\frac{\partial U}{\partial \tau} + \frac{\partial(U^2)}{\partial X} + \frac{\partial(UV)}{\partial Y} = -\frac{\partial P}{\partial X} + \frac{1}{Re} \left(\frac{\partial^2 U}{\partial X^2} + \frac{\partial^2 U}{\partial Y^2} \right) \quad (2)$$

$$\frac{\partial V}{\partial \tau} + \frac{\partial(UV)}{\partial X} + \frac{\partial(V^2)}{\partial Y} = -\frac{\partial P}{\partial Y} + \frac{1}{Re} \left(\frac{\partial^2 V}{\partial X^2} + \frac{\partial^2 V}{\partial Y^2} \right) \quad (3)$$

Energy equation:

$$\frac{\partial \theta}{\partial \tau} + \frac{\partial(U\theta)}{\partial X} + \frac{\partial(V\theta)}{\partial Y} = -\frac{\partial P}{\partial X} + \frac{1}{Pr Re} \left(\frac{\partial^2 \theta}{\partial X^2} + \frac{\partial^2 \theta}{\partial Y^2} \right) \quad (4)$$

The equations of conservation of mass and momentum in the case of isothermal, incompressible, stationary turbulence can be written in Cartesian-tensor notation as

$$\frac{\partial U_i}{\partial x_i} = 0 \quad (5)$$

$$U_j \frac{\partial U_i}{\partial x_j} = -\frac{1}{\rho} \frac{\partial p}{\partial x_i} + \frac{\partial}{\partial x_j} \left(\nu \left(\frac{\partial U_i}{\partial x_j} + \frac{\partial U_j}{\partial x_i} \right) - \overline{u_i' u_j'} \right) \quad (6)$$

where ρ is the fluid density, ν is the molecular viscosity and p is the static pressure,

2.3 Turbulence Models

2.3.1 Standard k- ϵ model

The equations of the model are [38]:

$$U_i \frac{\partial k}{\partial x_i} - \frac{\partial}{\partial x_i} \left[\frac{v_T}{\sigma_k} \frac{\partial k}{\partial x_i} \right] = P - \epsilon \quad (7)$$

$$U_j \frac{\partial \epsilon}{\partial x_j} - \frac{\partial}{\partial x_j} \left[\frac{v_T}{\sigma_\epsilon} \frac{\partial \epsilon}{\partial x_j} \right] = \frac{\epsilon}{k} (C_{\epsilon 1} P - C_{\epsilon 2} \epsilon) \quad (8)$$

$$v_T = C_\mu \frac{K^2}{\epsilon} \quad (9)$$

$$P_k = -\overline{u_i u_j} \left(\frac{\partial U_j}{\partial x_i} + \frac{\partial U_i}{\partial x_j} \right) \quad (10)$$

$$\overline{u_i u_j} = \frac{2}{3} \delta_{ij} k - v_T \left(\frac{\partial U_j}{\partial x_i} + \frac{\partial U_i}{\partial x_j} \right) \quad (11)$$

where C_μ , $C_{\epsilon 1}$, $C_{\epsilon 2}$, σ_k , and σ_ϵ are the model constants and v_T is the Boussinesq eddy viscosity. P_k represents the production rate of the turbulence kinetic energy. The values of that constants are $C_\mu = 0.09$, $C_{\epsilon 1} = 1.44$, $C_{\epsilon 2} = 1.92$, $\sigma_k = 1.0$, and $\sigma_\epsilon = 1.3$.

2.3.2 Realizable k- ϵ model

The equations of the model are [39]:

$$\frac{\partial(U_j \epsilon)}{\partial x_j} = \frac{1}{\rho} \left(\mu + \frac{\mu_t}{\sigma_\epsilon} \right) \nabla^2 \epsilon + \frac{1}{\rho} C_1 S_{\rho \epsilon} - C_2 \frac{\epsilon^2}{\sigma_k + \sqrt{v \epsilon}} \quad (12)$$

where $C_1 = \max[0.43, n/(n+5)]$, $C_2 = 1$, $\sigma_k = 1$, $\sigma_\epsilon = 1.2$, $n = Sk/\epsilon$

2.3.3 SST k- ω model

The equations of the model are [40]:

Turbulent Kinetic Energy:

$$U_i \frac{\partial k}{\partial x_i} = \frac{1}{\rho} P_k - k \omega \beta^* + \frac{1}{\rho} \frac{\partial}{\partial x_i} \left[(\mu + \sigma_K \mu_T) \frac{\partial k}{\partial x_i} \right] \quad (13)$$

Specific dissipation rate:

$$U_i \frac{\partial \omega}{\partial x_i} = \alpha S^2 - \beta \omega^2 + \frac{1}{\rho} \frac{\partial}{\partial x_i} \left[(\mu + \sigma_{\omega 1} \mu_T) \frac{\partial \omega}{\partial x_i} \right] + 2(1 - F_1) \sigma_{\omega 2} \frac{1}{\omega} \frac{\partial k}{\partial x_i} \frac{\partial \omega}{\partial x_i} \quad (14)$$

where F_1 is the blending function given by

$$F_1 = \tanh \left\{ \left\{ \min \left[\max \left(\frac{\sqrt{k}}{\beta^* \omega y}, \frac{500g}{y^2 \omega} \right), \frac{4\rho \sigma_{\omega 2} k}{CD_{k\omega} y^2} \right] \right\} \wedge 4 \right\} \quad (15)$$

with $CD_{k\omega} = \max\left(2\rho\sigma_{\omega 2} \frac{1}{\omega} \frac{\partial k}{\partial x_i} \frac{\partial \omega}{\partial x_i}, 10^{-10}\right)$ and y is the distance from the wall

The value of the blending function $F1$ is zero away from the wall, where the $k - \epsilon$ model is applicable while it is one in the boundary layer where $k - \omega$ is applicable. The turbulent eddy viscosity for the SST model is defined as follows.

$$g_T = \frac{a_1 k}{\max(a_1 \omega, SF_2)} \quad (16)$$

where S is the invariant measure of strain rate and $F2$ is a second blending function defined by

$$F_2 = \left[\tanh \left[\max \left(\frac{2\sqrt{k}}{\beta^* \omega y}, \frac{500g}{y^2 \omega} \right) \right]^2 \right] \quad (17)$$

A production limiter, used to prevent turbulence in stagnation regions, is given by

$$P_k = \mu_T \frac{\partial U_i}{\partial x_i} \left(\frac{\partial U_i}{\partial x_j} + \frac{\partial U_j}{\partial x_i} \right) \quad (18)$$

The constants are calculated by the combination of corresponding constants of $k-\omega$ and $k-\epsilon$ models. Wilcox [41] gives the values of constants for this model as:

$$\beta^* = 0.09, \alpha_1 = \frac{5}{9}, \beta_1 = \frac{3}{40}, \sigma_{k1} = 0.85, \sigma_{\omega 1} = 0.5, \alpha_2 = 0.44, \beta_2 = 0.0828, \sigma_{k2} = 1,$$

$$\sigma_{\omega 2} = 0.856$$

2.3 CFD Stimulations

Many parameters have been employed for use as criteria for flow characterization. In the turbulent flow, the behaviours that the researcher interested are vortices size, mean velocity profile and turbulent intensity. These parameters are being employed for differentiate one flow from another in different turbulence models. Due to simplicity, robustness, and wide industrial applications, the RANS model is used for computations. Two-equation family models: standard $k-\epsilon$, realizable $k-\epsilon$, and shear stress transport (SST) are considered. Numerical stimulation in this paper was aimed to investigate the mean velocity in x -axis and flow phenomena of the sudden expansion in pipe such as vortices size and turbulent intensity. The computational fluid dynamics software (FLUENT) with SIMPLE algorithm is used for the investigation. The iteration of the standard $k-\epsilon$, realizable $k-\epsilon$, and shear stress transport (SST) $k-\omega$ models are based on Reynolds averaged Navier Stokes equations.

3.0 RESULTS AND DISCUSSION

The main objective of this study is to investigate the performance of the three turbulence models in predicting the flow pattern, velocity profiles and turbulence intensity profiles in the case of turbulent diesel flow in pipe with sudden expansion. The advantages and disadvantages of each model are discussed.

3.1 Vortices Size

All turbulence models show similar general behaviour of the flow in pipe with sudden expansion. Figure 3 (a), 4(a),and 5(a)shows the flow pattern downstream from the step for three turbulence models. A main recirculating loop is clearly observed and in clockwise direction from the flow for three turbulence models. Downstream of the reattachment point, the flow at the wall has a downstream direction and a boundary layer develops.

The three turbulent models show different vortices size and strength in x-axis direction. The turbulence model which gave the best prediction in the sudden expansion geometry is shear stress transport (SST) $k-\omega$ model shown in Figure 5(a). This result is in compliance with the theory which SST $k-\omega$ model can use to predict the complex boundary layer flows under adverse pressure gradient and separation. The realizable $k-\epsilon$ model provided the moderate results shown in Figure 4 (a). The vortices form from the step in realizable $k-\epsilon$ model is smaller and less obvious compared to SST $k-\omega$ model. The standard $k-\epsilon$ model is performs poorly for flows under severe pressure gradient and separation. Figure 3 (a) shows the small vortices form after the step region.

3.2 Mean velocity profile

All three standard $k-\epsilon$, realizable $k-\epsilon$, and shear stress transport (SST) $k-\omega$ models, show the changes in the velocity at different locations, including the reversal flow near the step. These turbulent models indicated the mean velocity profile at $X/H=4, 6, 8, 12$ and 16 . Furthermore, each of the models demonstrated that velocity near to the wall is low and become high when far away from wall. This happens because of friction and shear stress at wall. Among the three turbulent models, SST $k-\omega$ model show the highest mean velocity after the step which include forward velocity and reverse velocity.

The mean velocity profile of standard $k-\epsilon$ model as shown in Figure 3(b) indicated that there is a large velocity gradient at $X/H=4$ and the flow is in high turbulent conditions. The intensity of turbulent is become less from $X/H=4$ to $X/H=12$ and finally in stagnant condition. The turbulent flow still can observed clearly at $X/H=6$ and it intensity slowly reduce at $X/H=8$. The flow at $X/H=16$ is almost stagnant and less turbulent.

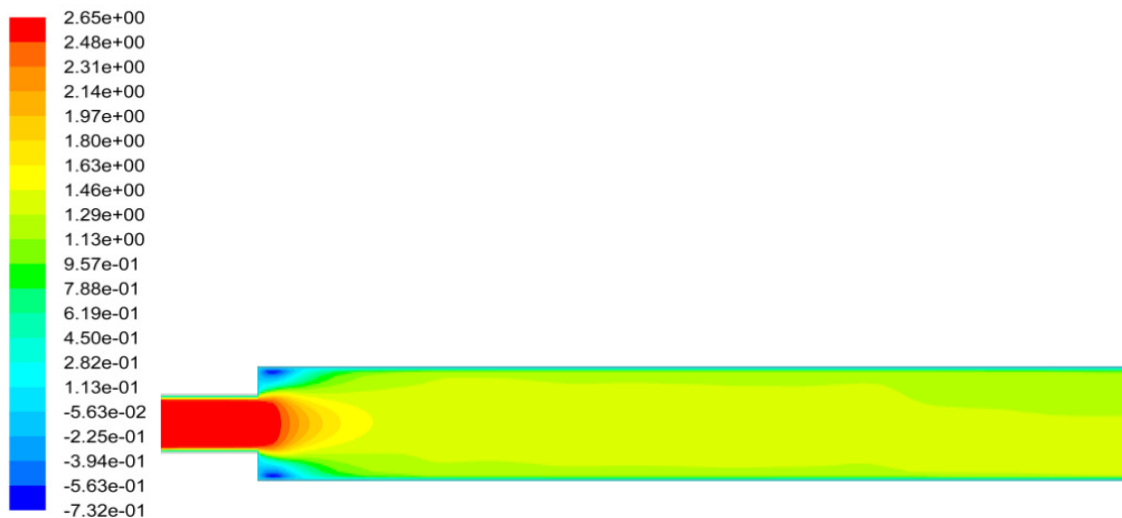


Figure 3(a): Contours of x-axis direction velocity for standard $k-\epsilon$ model (m/s)

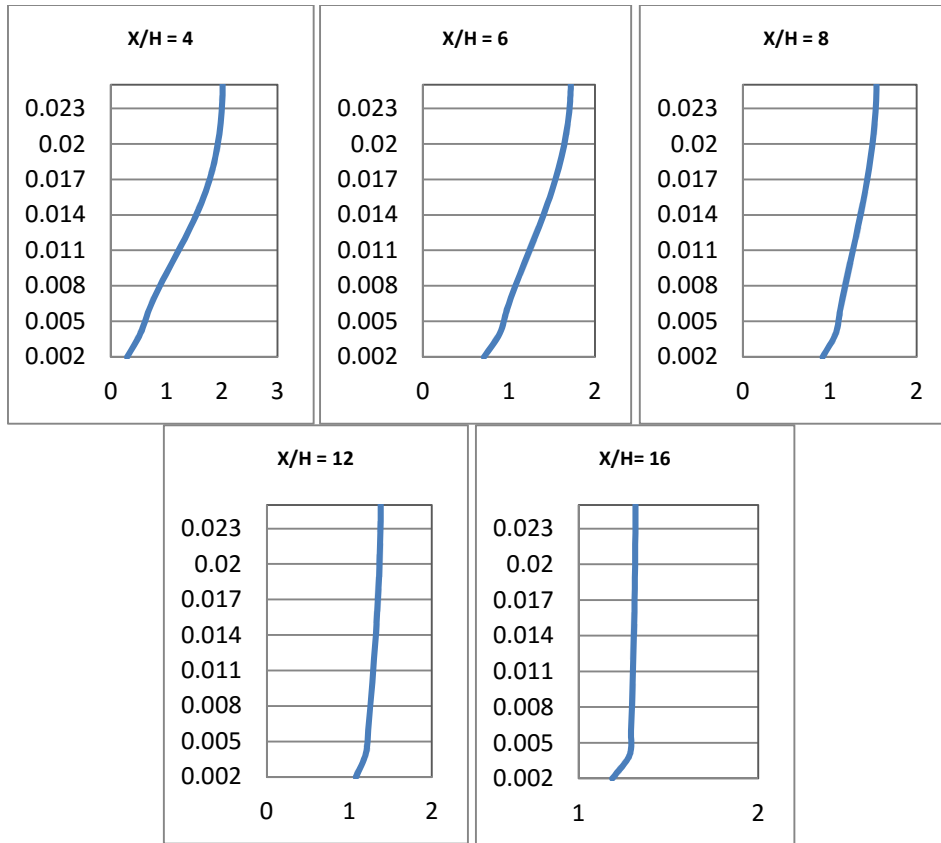


Figure 3(b): Velocity in x-axis direction for standard k-ε model (m/s)

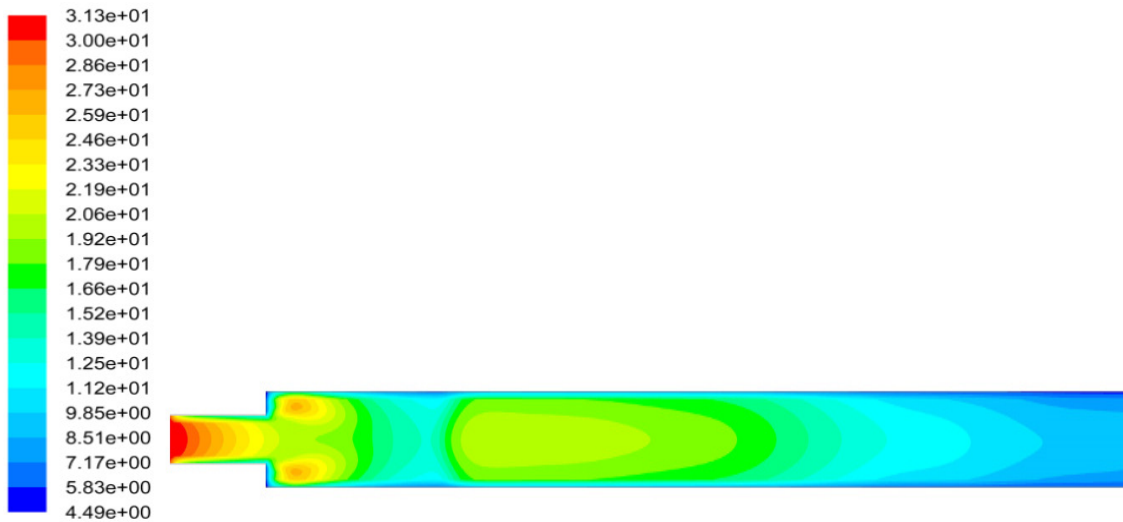


Figure 3(c): Contours of turbulent intensity for standard k-ε model (%)

The mean velocity profile of realizable k-ε model as shown in Figure 4(b) indicated that there is a large velocity gradient at $X/H=4$ and the flow is in high turbulent conditions. The intensity of turbulent and velocity of this model is higher compared to the standard k-ε model at $X/H=4$. There are maximum reverse velocity in this axial distance and this reverse velocity cause the vortices form. The intensity of turbulent is become less from $X/H=4$ to $X/H=12$ and finally in stagnant condition. The turbulent flow still can observed clearly at $X/H=6$ and it intensity slowly reduce at $X/H=16$. The flow at $X/H=16$ is almost stagnant and less turbulent.

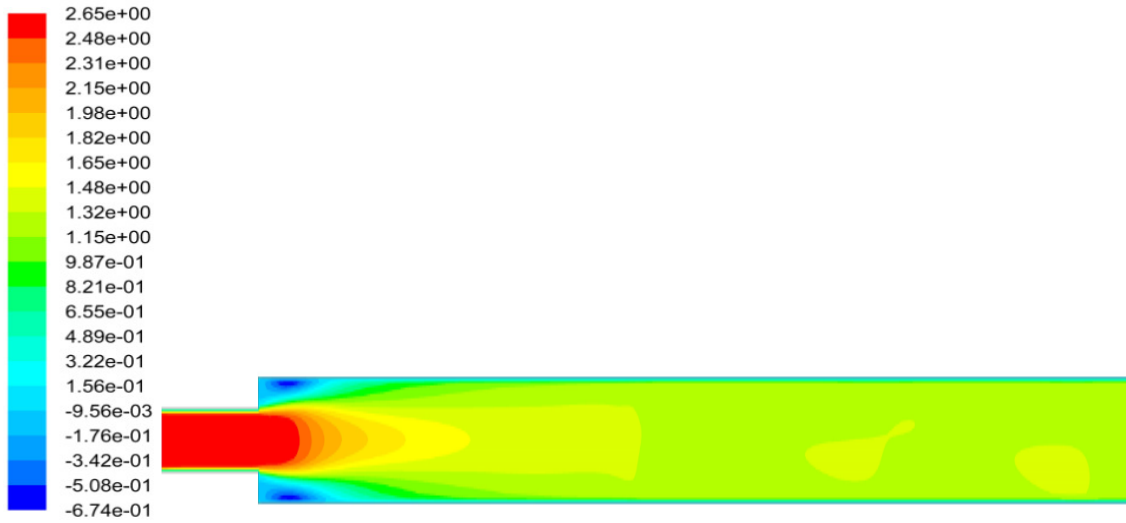


Figure 4(a): Contours of x-axis direction velocity for realizable $k-\epsilon$ model (m/s)

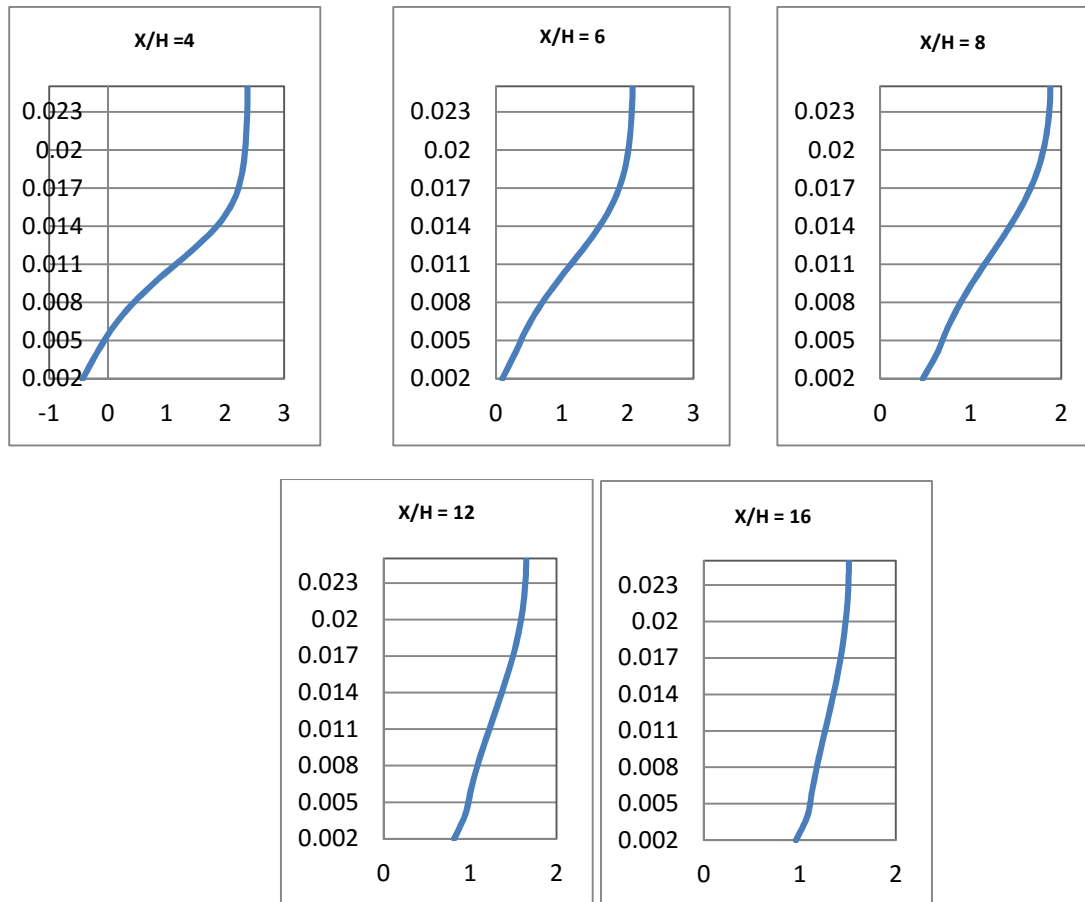


Figure 4(b): Velocity in x-axis direction for realizable $k-\epsilon$ model (m/s)

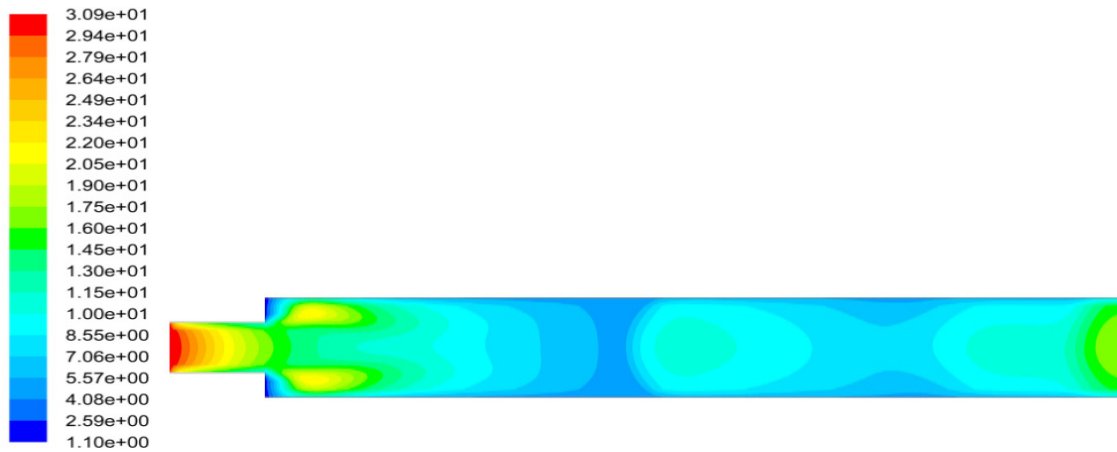


Figure 4(c): Contours of turbulent intensity for realizable $k-\epsilon$ model (%)

The mean velocity profile of SST $k-\omega$ model shown in Figure 5(b) indicated that there is a large velocity gradient at $X/H=4$ and the flow is in high turbulent conditions. The intensity of turbulent and velocity of this model is higher compared to the realizable $k-\epsilon$ model at $X/H=4$. There are maximum reverse velocity in this axial distance and this reverse velocity cause the vortices form. The intensity of turbulent is become less from $X/H=4$ to $X/H=12$ and finally in stagnant condition. The turbulent flow and reverse velocity still can observed clearly at $X/H=6$ and it intensity slowly reduce at $X/H=12$. The flow at $X/H=16$ is almost stagnant and less turbulent.

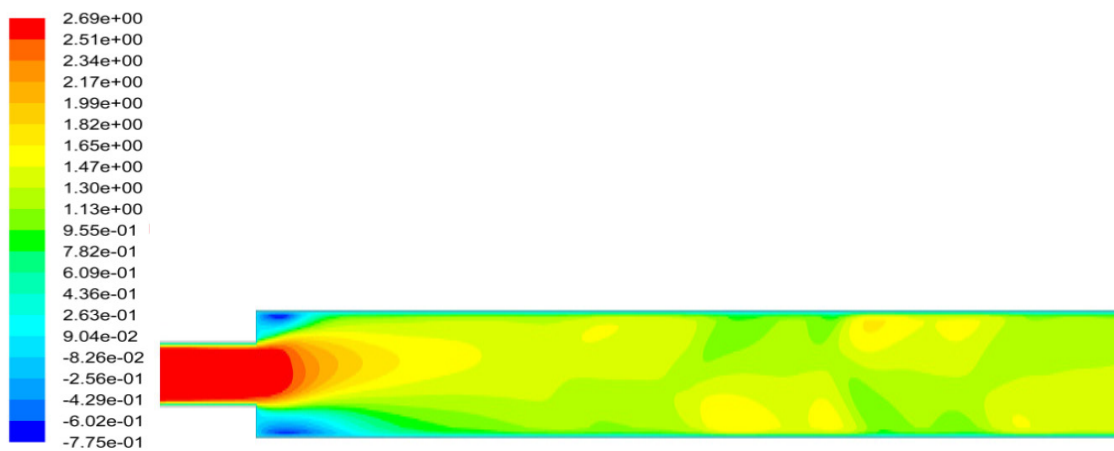


Figure 5(a): Contours of x-axis direction velocity for SST $k-\omega$ model (m/s)

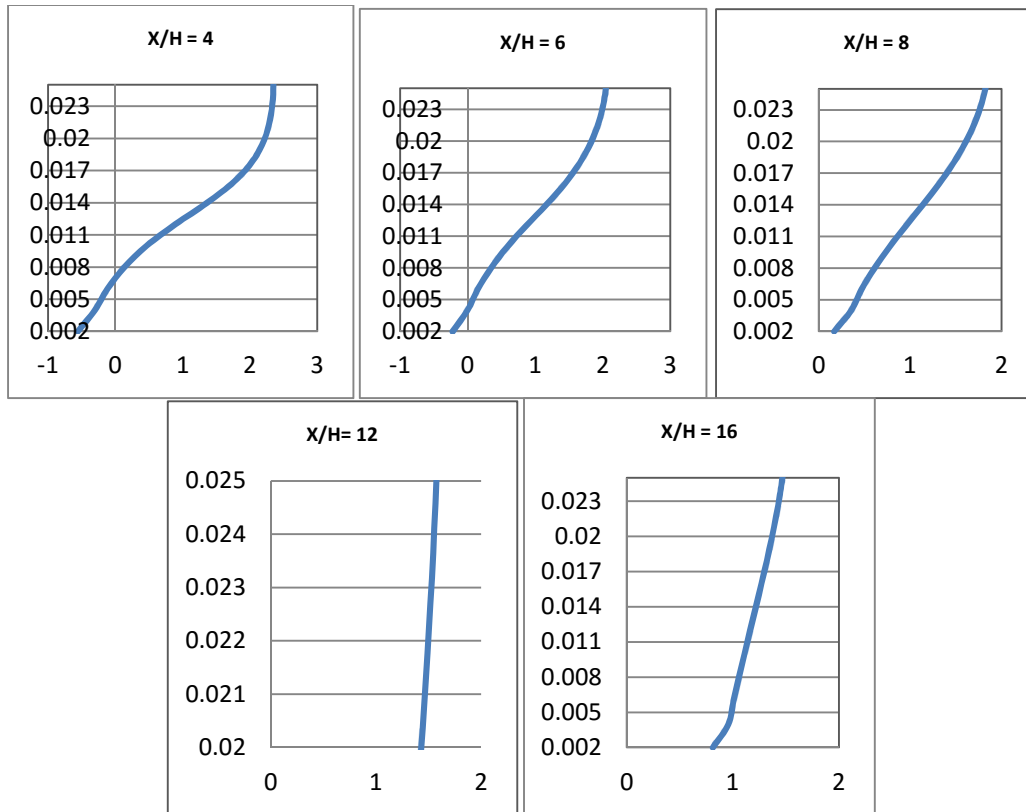


Figure 5(b): Velocity in x-axis direction for SST $k-\omega$ model (m/s)

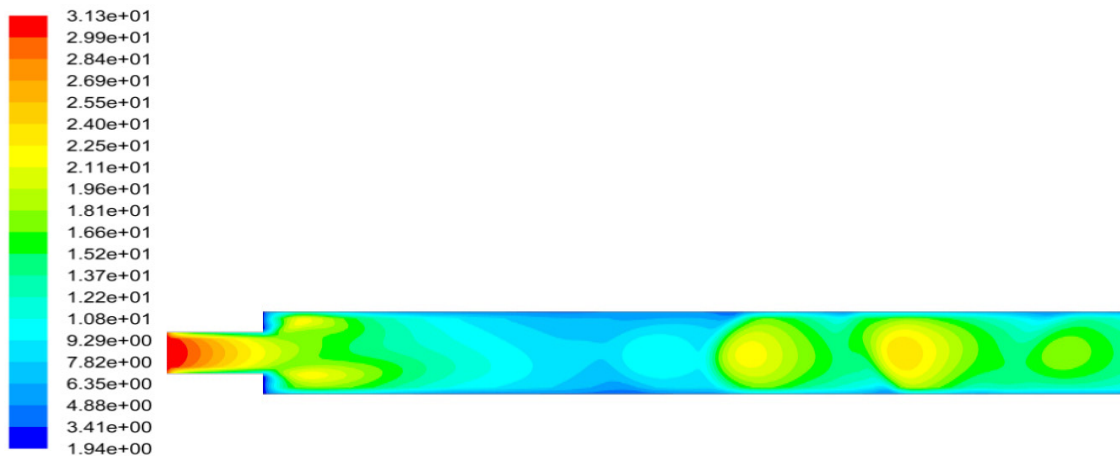


Figure 5 (c): Contours of turbulent intensity for SST $k-\omega$ model (%)

3.3 Turbulence intensity

The turbulence intensity pattern of these three turbulence model shown in Figure 3(c), 4(c), and 5(c) are almost same and follow the trend that high at inlet and after the step but low at the outlet of the pipe. The turbulence intensity of standard $k-\epsilon$ model is high at the inlet and after the step. But turbulence intensity become lower when far away from the inlet and finally become lowest at the outlet of the pipe. The turbulence intensity of realizable $k-\epsilon$ model is lower after the step and higher at the outlet compared to standard $k-\epsilon$ model. The turbulent intensity for SST $k-\omega$ model is higher near to outlet of the pipe compared to realizable $k-\epsilon$ model.

3.4 Validation of Results

The present numerical results were validated against the results of experiment about investigation of flow characteristic in pipe with sudden expansion. The stimulation results of standard $k-\epsilon$, realizable $k-\epsilon$, and shear stress transport (SST) $k-\omega$ models are compared to the experimental data of Founti and Klipfel [11] shown in Figure 6. The trends of mean velocity profile of these three models are same as the experimental data. As compared to the region away from the wall, the near wall region and the flow reattachment are in good agreement with the experimental results. The velocities are high near to the inlet of the pipe and then slowly reduce to some level. Finally, the velocities are low and stagnant at the outlet of the pipe.

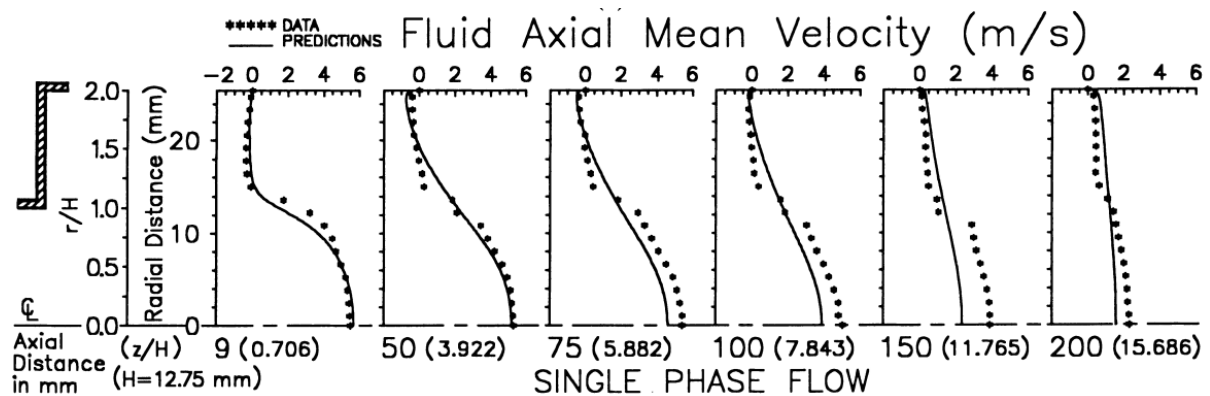


Figure 6: Experimental data of fluid axial mean velocity.

4.0 CONCLUSION

The stimulation of turbulence flow was conducted by a sudden expansion duct with Reynolds number of 20000 at the inlet of the solution and expansion ratio of 1:2. The three turbulence flow models, standard $k-\epsilon$, realizable $k-\epsilon$, and SST $k-\omega$ were considered. The flow patterns after the step in pipe with sudden expansion were successfully shown by the numerical results. Among three turbulence models, SST $k-\omega$ model shows the best prediction results in terms of recirculation size and velocity profile. Besides that, the three turbulence models show trends of the mean velocity profile same as experimental data.

REFERENCES

- [1] J.D. Anderson, L.J. Clancy, Introduction to Flight, Section 4.20, Aerodynamics, Section 4.14, 2004.
- [2] B. Tocher, Bifurcation contrasts between plane Poiseuille flow and plane magnetohydrodynamic flow, Doctor of Philosophy, Aston University, 2013.
- [3] P.K. Chang, Separation of Flow, 1st edition, Headington Hill Hall, 1970.
- [4] W.T. Ashurst, F. Durst, C. Tropea, Two-dimensional separated flow: experiment and discrete vortex dynamic simulation, In: Symposium on Computation of Viscous Inviscid Interactions, Colorado Springs, CO, USA, 1980.

- [5] P.K. Chang, Control of Flow Separation: Energy Conservation, Operational Efficiency and Safety, McGraw-Hill Book Co., New York, 1976
- [6] D.C. Wilcox, Basic Fluid Mechanics, 3rd edition, Mill Valley: DCW Industries Inc., 1980, 664-668.
- [7] M. Kiya, O. Mochizuki, H. Ishikawa, Challenging Issues in Separated and Complex Turbulent Flows, Hokkaido University, Japan, 1975.
- [8] L. Khezzar, J.H. Whitelaw, M. Yianneskis, An experimental study of round sudden expansion flows, in: Proceedings of the Fifth Symposium on turbulent shear flows, Cornell University, 1985, pp. 5-25.
- [9] L. Back, E. Rosshke, Shear layer regimes and wave instabilities and reattachment lengths downstream of an abrupt circular sudden expansion, Journal of Applied Mechanics 94 (1972) 677-681.
- [10] M. Stieglmeier, C. Tropea, N. Weiner, W. Nitsche, Experimental investigation of the flow through axisymmetric expansions, Journal of Fluids Engineering 111 (1989) 464-471.
- [11] M. Founti, A. Klipfel, Experimental and computational investigations of nearly dense two-phase sudden expansion flows, Experimental Thermal and Fluid Science 17 (1998) 27-36.
- [12] D.M. Driver, H.L. Seegmiller, Features of a reattaching turbulent shear layer in divergent channel flow, AIAA Journal 23 (1983) 163-171
- [13] M.C. Celenligil, G.I. Mellor, Numerical solution of two-dimensional turbulent separated flows using a Reynoldsstress closure model, ASME, 1985, Paper No. 85-WA/FE-5.
- [14] R.J. Goldstein, V.L. Eriksen, R.M. Olsen, E.R.G. Eckert, Laminar separation, reattachment and transition of the flow over a downstream-facing step, Journal of Heat Transfer, ASME Transactions 92 (1970) 732-741.
- [15] J.O. Paulo, Asymmetric flows of viscoelastic fluids in symmetric planar expansion geometries, Journal of Non-Newtonian Fluid Mechanics 114 (2003) 33-63.
- [16] J. Laufer, The structure of turbulence in fully developed pipe flow, NACA report no. 1174.
- [17] O.F. Vasilev, N.F. Budunov, Calculation of flow turbulence in the presence of sudden expansion of the channel, Fluid Mechanics - Soviet Research 5 (1976) 156-161.
- [18] B.E. Launder, D.B. Spalding, The Numerical Computation of Turbulent Flows, Computer Methods in Applied Mechanics and Engineering 3 (1974) 269-289.

- [19] M.C. Chaurvedi, Flow characteristics of axisymmetric expansion, Journal of the Hydraulic Division, Proceeding of the American Society of Civil Engineers 89 (1963) 61-92.
- [20] R. Smyth, Turbulent flow over a plane symmetric sudden expansion, Journal of Fluids Engineering 101 (1979) 348-353.
- [21] R.D. Gould, W.H. Stevenson, H.D. Thompson, Investigation of Turbulent Transport in an Axisymmetric Sudden Expansion, American Institute of Aeronautics and Astronautics Journal 28 (1990) 276-283.
- [22] K. Mohanaragam, J.Y. Tu, L. Chen, Numerical study of particle dispersion behind sudden expansion geometry and its effect on step heights, Computers and Chemical Engineering 32 (2008) 3187-3197.
- [23] W.H. Stevenson, H.D. Thompson, R.R. Craig, Laser velocimeter measurements in highly turbulent recirculating flows, Journal of Fluids Engineering 106 (1984) 173-180.
- [24] R.P. Durrett, W.H. Stevenson, H.D. Thompson, 1988. Radial and axial turbulent flow measurements with an LDV in an axisymmetric sudden expansion air flow, Journal of Fluid Engineering 1 (10) (1988) 367-372.
- [25] R.D. Gould, W.H. Stevenson, H.D. Thompson, Investigation of turbulent transport in an axisymmetric sudden expansion, American Institute of Aeronautics and Astronautics Journal 28 (1990) 276-283
- [26] W.J. Devenport, E.P. Sutton, An experimental study of two flows through an axisymmetric sudden expansion, Experimental Fluids 14 (1993) 423-432
- [27] R.G. Teyssandier, M.P. Wilson, An analysis of flow through sudden enlargements in pipes, Journal of Fluid Mechanics 64 (1974) 85-96.
- [28] C.E. Tinney, M.N. Glauser, E.L. Eaton, J.A. Taylor, Low dimensional azimuthal characteristics of suddenly expanding axisymmetric flows, Journal of Fluid Mechanics 567 (2006) 141-155.
- [29] B. Guo, T.A.G. Langrish, D.F. Fletcher, Numerical simulation of unsteady turbulent flow in axisymmetric sudden expansions, Journal of Fluids Engineering 123 (2001) 574-587.
- [30] B.F. Armaly, F. Durst, J.C.F. Pereira, B. Schonung, Experiment and Theoretical Investigation of back-ward facing step flow, Journal of Fluid Mechanics 127 (1983) 473-496.
- [31] M. Stieglmeier, C. Tropea, N. Weiner, W. Nitsche, Experimental investigation of the flow through axisymmetric expansion, Journal of Fluid Engineering 111 (1989) 464-471.

- [32] D.R. Cole, M.N. Glauser, Utilizing a flying hot-wire system to study the flow in an Axi-symmetric sudden expansion, *Experimental Thermal and Fluid Sciences* 18 (1998) 150-167.
- [33] C. Mistrangelo, L. Buhler, Numerical Investigation of liquid metal flows in Rectangular Sudden Expansions, *Fusion Engineering and Design* 82 (2007) 2176-2182.
- [34] L.W. Signrdson, The structure and control of a turbulent reattaching flow, *Journal of Fluid Mechanics* 298 (1995) 139-165.
- [35] S.R.N. De Zilwa, L. Khezzar, J.H. Whitelaw, Flow through plane sudden expansions, *International Journal for Numerical Methods in Fluids* 32 (2000) 313-329.
- [36] Canbazoğlu, Suat, Bozkir, Oğuz, Analysis of pressure distribution of turbulent asymmetric flow in a flat duct symmetric sudden expansion with small aspect ratio, *Fluid Dynamic Research* 35 (5) (2004) 341-355.
- [37] E.D. Koronaki, H.H. Liakos, M.A. Founti, N.C. Markatos, Numerical study of turbulent diesel flow in a pipe with sudden expansion, *Applied Mathematical Modelling* 25 (2001) 319-333.
- [38] B.E. Launder, D.B. Spalding, The numerical computation of turbulent flow, *Computer Methods in Applied Mechanics and Engineering* 3 (1974) 269.
- [39] P. Rohdin, B. Moshfegh, Numerical predictions of indoor climate in large industrial premises: A comparison between different k- ϵ models supported by field measurements, *Building and Environment* 42 (2007) 3872-3882.
- [40] R.F. Menter, Two equation eddy viscosity turbulence models for engineering applications, *American Institute of Aeronautics and Astronautics Journal* 32 (8) (1994) 269 - 289.
- [41] D.C. Wilcox, *Turbulence modelling for CFD*, DCW Industries Inc., La Canada, CA, 2006.